



Article

Uncommon Polyketides from *Penicillium steckii* AS-324, a Marine Endozoic Fungus Isolated from Deep-Sea Coral in the Magellan Seamount

Xue-Yi Hu^{1,2,3}, Xiao-Ming Li^{1,2} , Bin-Gui Wang^{1,2,3,4,*} and Ling-Hong Meng^{1,2,4,*}

- ¹ CAS and Shandong Province Key Laboratory of Experimental Marine Biology, Institute of Oceanology, Chinese Academy of Sciences, Nanhai Road 7, Qingdao 266071, China; xueyihu61@163.com (X.-Y.H.); lixmqd@qdio.ac.cn (X.-M.L.)
- ² Laboratory of Marine Biology and Biotechnology, Qingdao National Laboratory for Marine Science and Technology, Wenhai Road 1, Qingdao 266237, China
- ³ College of Marine Science, University of Chinese Academy of Sciences, Yuquan Road 19A, Beijing 100049, China
- ⁴ Center for Ocean Mega-Science, Chinese Academy of Sciences, Nanhai Road 7, Qingdao 266071, China
- * Correspondence: wangbg@ms.qdio.ac.cn (B.-G.W.); menglh@ms.qdio.ac.cn (L.-H.M.); Tel.: +86-532-8289-8553 (B.-G.W.); +86-532-8289-8890 (L.-H.M.)

Abstract: Four unusual steckwaic acids E–H (1–4), possessing a rarely described acrylic acid unit at C-4 (1–3) or a double bond between C-12 and C-13 (4) are reported for the first time, along with four new analogues (5–8) and two known congeners (9 and 10). They were purified from the organic extract of *Penicillium steckii* AS-324, an endozoic fungus obtained from a deep-sea coral *Acanthogorgia* sp., which was collected from the Magellan Seamount at a depth of 1458 m. Their structures were determined by the interpretation of NMR and mass spectroscopic data. The relative and absolute configurations were determined by NOESY correlations, X-ray crystallographic analysis, and ECD calculations. All compounds were tested for their antimicrobial activities against human- and aquatic-pathogenic bacteria and plant-related pathogenic fungi.

Keywords: marine endozoic fungus; *Penicillium steckii*; polyketide derivatives; natural products; structure elucidation; biological activity



Citation: Hu, X.-Y.; Li, X.-M.; Wang, B.-G.; Meng, L.-H. Uncommon Polyketides from *Penicillium steckii* AS-324, a Marine Endozoic Fungus Isolated from Deep-Sea Coral in the Magellan Seamount. *Int. J. Mol. Sci.* **2022**, *23*, 6332. <https://doi.org/10.3390/ijms23116332>

Academic Editor: Miguel Angel Prieto Lage

Received: 30 April 2022

Accepted: 28 May 2022

Published: 6 June 2022

Publisher's Note: MDPI stays neutral with regard to jurisdictional claims in published maps and institutional affiliations.



Copyright: © 2022 by the authors. Licensee MDPI, Basel, Switzerland. This article is an open access article distributed under the terms and conditions of the Creative Commons Attribution (CC BY) license (<https://creativecommons.org/licenses/by/4.0/>).

1. Introduction

Deep-sea-living organisms have evolved under extreme environmental conditions, which have influenced the development of various biochemical functions compared to those living in shallow-water organisms [1,2]. Although the area of deep-sea habitats is much larger than that of shallow-sea habitats, compounds isolated from deep-sea organisms accounted for only ~2% of the more than 30,000 marine natural products [3,4], whereas approximately 75% of these molecules exhibited notable bioactivities. Improved technological capacity for sampling from the deep-sea environment has improved the discovery of deep-sea-derived natural products. In recent years, the number of deep-sea-sourced natural products increased rapidly, and these compounds usually display high bioactivity hits in bioassays [5]. Although the nature of the associations between a host and its associated microbes is far from understood, there is growing evidence that some coral-associated fungi have adopted the ability to produce secondary metabolites that are structurally divergent from their terrestrial counterparts [6–8]. Marine animal-related fungi often produce bioactive metabolites that might be interpreted as chemically mediated defense mechanisms to protect their host organisms from environmental hazards such as predation and pathogenic invasion [9]. Some studies have reported on the isolation of marine coral-associated *Penicillium* spp. as producers of bioactive metabolites [10–12].

Following our ongoing research about secondary metabolites from marine-derived fungi collected from deep-sea habitats [13,14], an endozoic fungus *Penicillium steckii* AS-324, obtained from the fresh tissues of deep-sea coral *Acanthogorgia* sp. collected from Magellan seamount in the Western Pacific Ocean at a depth of 1458 m, was cultured and chemically investigated. *P. steckii* has recently been proved to be an excellent source of antibacterial compounds based on genome sequencing and mining, as well as antibacterial screening of the crude extracts [15]. Eight new tanzawaic acid derivatives (1–8), together with two known analogues, tanzawaic acid H (9) [16] and tanzawaic acid S (10) [17], were isolated and identified. We recently reported 10 new tanzawaic acid derivatives, including steckwaic acids A–D from *P. steckii* AS-324 [18]. Further work on the remaining portions of this fungus resulted in the characterization of eight new (1–8) and two known (9 and 10) tanzawaic acid analogues (Figure 1). Among these compounds, steckwaic acids E–G (1–3) possess a rarely described acrylic acid unit at C-4, while compound 4 has a double bond at C-12, which is uncommon among the reported tanzawaic acids [16–18]. Details of the isolation, structure elucidation, and antimicrobial activity of compounds 1–10 are described herein.

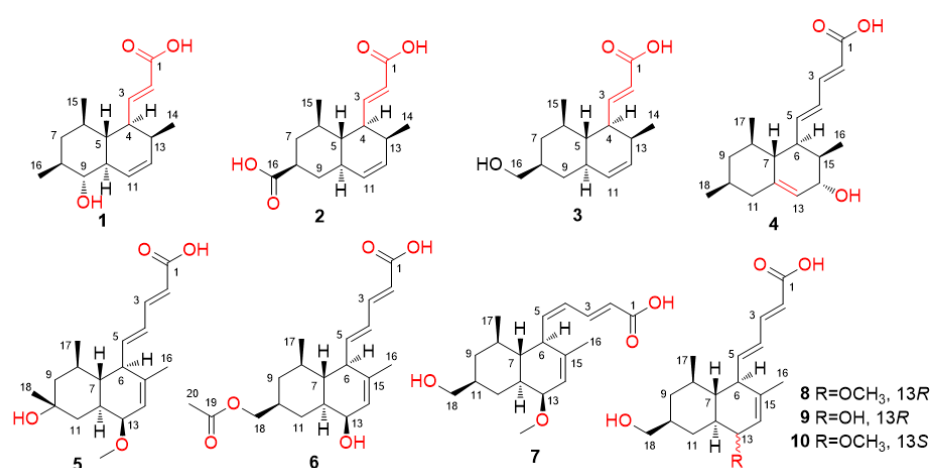


Figure 1. Structures of compounds 1–10.

2. Results

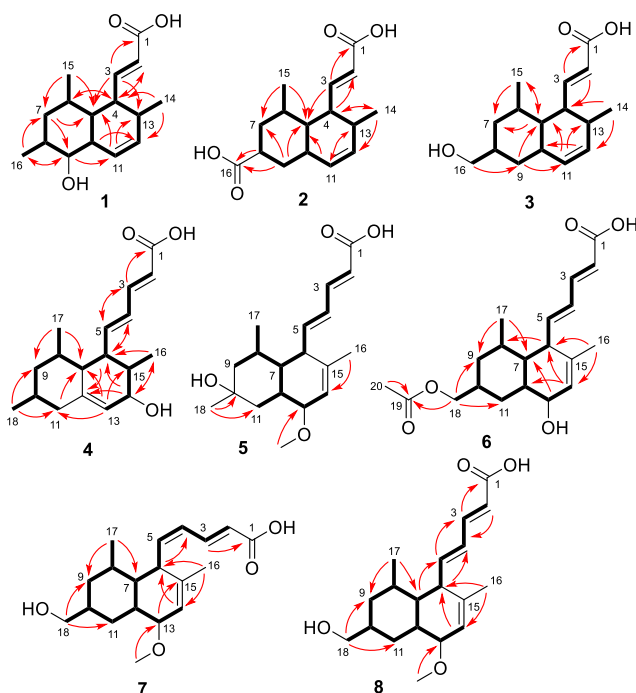
The culture of *P. steckii* AS-324 was extracted with EtOAc to gain the organic extract, which was then fractionated and purified by various chromatographic methods to yield compounds 1–10 (Figure 1).

Steckwaic acid E (1) was initially obtained as a white amorphous powder, and the molecular formula was assigned as C₁₆H₂₄O₃ by negative HRESIMS data. The ¹H and ¹³C NMR data (Table 1) revealed the presence of three doublet methyl substitutions, one methylene, eleven methines (with one oxygenated and four olefinic), and one carboxyl carbon. A large spin system incorporating H-2 through H-13 and three methyls, H₃-14, H₃-15, and H₃-16, confirmed the presence of a decalin skeleton with three methyl-substitution at C-6, C-8, and C-13 (Figure 2). HMBC correlations from H-3 to C-1, C-5, and C-13 and from H-2 to C-4 indicated the position of one acrylic acid side chain at C-4 (Figure 2). The large coupling constant between H-2 and H-3 (*J* = 15.4 Hz) suggested the *E*-geometry of the double bond, whereas the smaller coupling constant between H-11 and H-12 (*J* = 9.8 Hz) revealed the *Z*-geometry. Thus, the planar structure of 1 was determined. The coupling constants between H-4 and H-5, between H-5 and H-10, and between H-8 and H-9, as well as between H-9 and H-10, were all 9.5 Hz, indicating the *trans*-orientation of these adjacent proton pairs in the cyclohexane/cyclohexene units. NOESY correlations from H-3 to H-5 and H₃-15, as well as from H-5 to H-9, demonstrated them on the same face of these protons, while correlations from H-10 to H-6, H-8, and H-13 placed them on the opposite side (Figure 3).

Table 1. ^1H and ^{13}C NMR data of compounds 1–3 in $\text{DMSO-}d_6$.

No.	1		2		3	
	δ_{C} , Type	δ_{H} (J in Hz)	δ_{C} , Type	δ_{H} (J in Hz)	δ_{C} , Type	δ_{H} (J in Hz)
1	167.6, C		167.4, C ^a		167.6, C	
2	120.5, CH	5.71, d (15.4)	120.1, CH ^b	5.74, d (15.3)	120.5, CH	5.71, d (15.4)
3	154.2, CH	6.84, dd (15.4, 10.9)	154.2, CH	6.88, dd (15.3, 10.9)	153.2, CH	6.86, dd (15.4, 10.9)
4	48.0, CH	2.46, ddd (10.9, 9.5, 5.6)	47.5, CH	2.46, td (10.9, 5.0)	47.2, CH	2.45, td (10.9, 5.4)
5	44.9, CH	1.00, q (9.5)	46.0, CH	0.98, m	46.3, CH	0.88, overlap
6	35.8, CH	2.11, m	35.7, CH	1.37, m	35.4, CH	1.32, dddq (10.5, 10.1, 3.2, 6.4)
7	44.4, CH ₂	1.56, dt (13.7, 3.8) 0.83, overlap	40.0, CH ₂	1.81, overlap 1.11, overlap	40.5, CH ₂	1.66, dq (14.3, 3.2) 0.72, overlap
8	40.0, CH	1.35, overlap	43.2, CH	2.35, m	40.0, CH	1.52, m
9	77.0, CH	2.59, t (9.5)	35.4, CH ₂	1.93, d (12.3) 1.11, overlap	35.8, CH ₂	1.77, overlap 0.72, overlap
10	49.2, CH	1.67, td (9.5, 2.0)	41.5, CH	1.81, overlap	41.6, CH	1.77, overlap
11	129.4, CH	6.01, dt (9.8, 2.0)	131.7, CH	5.45, br d (9.7)	131.8, CH	5.44, dt (9.6, 2.0)
12	132.2, CH	5.58, ddd (9.8, 4.3, 2.0)	132.6, CH	5.58, br d (9.7)	131.9, CH	5.56, ddd (9.6, 4.4, 2.0)
13	36.1, CH	1.35, overlap	36.7, CH	2.15, q (6.1)	36.3, CH	2.14, m
14	16.6, CH ₃	0.88, d (7.1)	16.5, CH ₃	0.90, overlap	16.1, CH ₃	0.90, d (7.0)
15	22.3, CH ₃	0.83, overlap	22.6, CH ₃	0.90, overlap	22.5, CH ₃	0.88, d (6.4)
16	19.2, CH ₃	0.91, d (6.4)	176.9, C ^a		66.3, CH ₂	3.20, m
1-COOH		12.09, br s		12.02, br s		
9-OH		4.56, br s				

^a Detected by HMBC data. ^b Detected by HSQC data.

**Figure 2.** Key COSY (bold lines) and HMBC (arrows) correlations of compounds 1–8.

To unambiguously confirm the structure and configuration of compound **1**, attempts to cultivate quality crystals were performed, and suitable crystals were obtained by dissolving the samples in MeOH and refrigerating them to evaporate the solvent slowly. Single-crystal X-ray diffraction analysis using Cu K α radiation confirmed the structure of **1**, and the absolute configuration was 4*S*, 5*R*, 6*R*, 8*S*, 9*R*, 10*R*, and 13*S* with the Flack parameter $-0.09(13)$ (Figure 4).

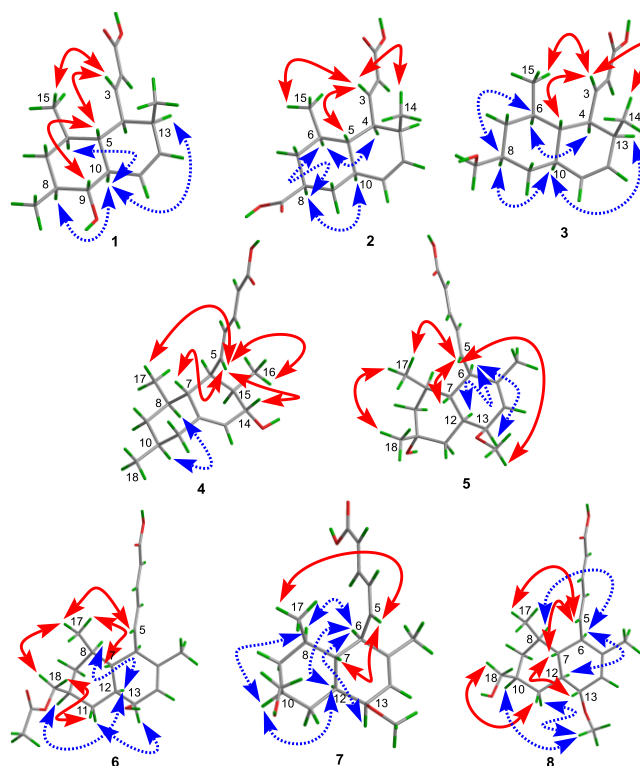


Figure 3. Key NOESY correlations of compounds 1–8.

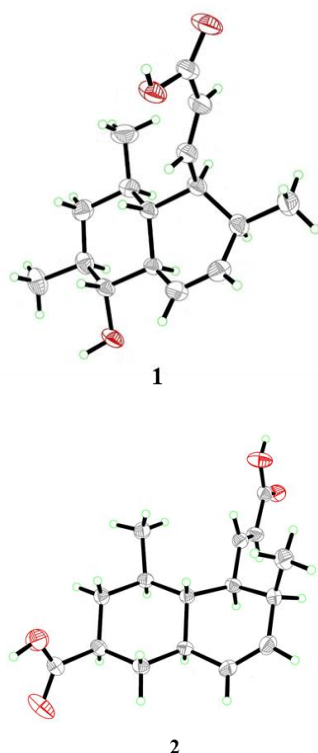


Figure 4. X-ray crystallographic structures of compounds 1 and 2 (with a thermal ellipsoid probability of 50%).

Steckwaic acid F (**2**), obtained as colorless crystals, was assigned a molecular formula of $C_{16}H_{22}O_4$ according to the HRESIMS analysis. Detailed inspection of its NMR data revealed the same skeleton as that of compound **1**, and the main differences are that the oxygenated methine resonating at δ_C/δ_H 77.0/2.59 (CH-9) in **1** was replaced by methylene

resonating at δ_C/δ_H 35.4/1.93 and 1.11 (CH₂-9) in **2**, whereas a carboxyl carbon resonating at δ_C 176.9 (C-16) was observed by HMBC in **2**, which replaced the methyl group resonating at δ_C/δ_H 19.2/0.91 (CH₃-16) in **1**. The large spin system similar to that in **1** was otherwise intact, albeit with some chemical shift differences and the absence of the methyl group CH₃-16 in **2** (Figure 2). HMBC correlations from H-8 and H-9 to the carboxyl carbon C-16, as well as from H-9 to C-5 and C-7, confirmed the planar structure of compound **2** (Figure 2). The coupling constant between H-2 and H-3 ($J = 15.3$ Hz) suggested the *E*-geometry of the double bond. NOE correlations from H-3 to H-5, H₃-14, and H₃-15 suggested the protons were in the same orientation, whereas correlations from H-6 to H-4 and H-8 as well as from H-8 to H-10 positioned them on the other side (Figure 3). The structure and absolute configuration of compound **2** were confirmed by X-ray diffraction analysis using Cu K α radiation, and the Flack parameter 0.05(10) permitted assignment of the absolute configuration as 4*S*, 5*S*, 6*R*, 8*S*, 10*R*, and 13*S* (Figure 4).

Steckwaic acid G (**3**), obtained as a white amorphous powder, was assigned the molecular formula C₁₆H₂₄O₃ by HRESIMS and NMR data. The chemical structure of compound **3** was almost identical to that of **2**. The main difference between **3** and **2** was evident in the nonappearance of one of the two carboxyl carbons C-16 (δ_C 176.9 in **2**) in the ¹³C-NMR spectrum of **3**, the appearance of ¹H- and ¹³C-NMR resonances for an oxymethylene moiety CH₂-16 (δ_C 66.3 and δ_H 3.20 in **3**), and the related changes in chemical shifts and multiplicities of nearby carbons and protons around CH-9 (Table 1). This spectral evidence suggests that the carboxyl carbon C-16 in **2** was reduced to form an oxymethylene unit in **3**, and this assignment was further confirmed by COSY and HMBC correlations (Figure 2). The coupling constant between H-2 and H-3 ($J = 15.4$ Hz) was similar to that observed in compound **2**, which indicated the *E*-geometry of the double bond at C-2. NOESY correlations from H-3 to H-5, H₃-14, and H₃-15 supported the cofacial orientation of these protons, while correlations from H-6 to H-4 and H-8, as well as from H-10 to H-8 and H-13, placed these groups on the opposite face (Figure 3). The ECD spectrum of **3** closely matched that of **1** and **2**, which showed the same positive cotton effects near 225 nm (Figure 5), enabling the assignment of the absolute configurations of compound **3** as 4*S*, 5*S*, 6*R*, 8*S*, 10*R*, and 13*S*.

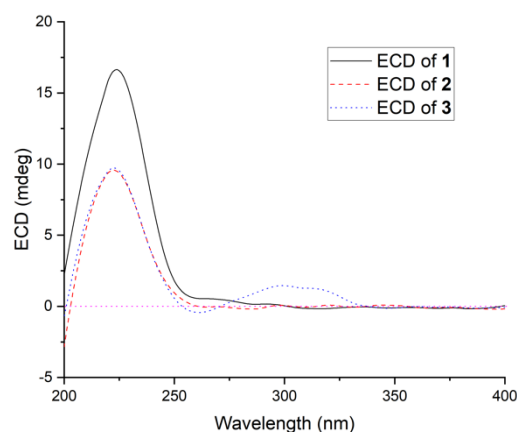


Figure 5. ECD spectra of compounds **1–3**.

Steckwaic acid H (**4**) was determined to have the molecular formula C₁₈H₂₆O₃ based on the negative HRESIMS data. Its NMR data (Table 2) displayed typical signals of a decalin skeleton with three methyl signals for C-8, C-10, and C-15, and the appropriately modified acrylic acid substituent in **1–3** was changed to a penta-2,4-dienoic acid moiety in **4**. HMBC correlations from the olefinic proton H-13 to C-7, C-11, and C-15, as well as from H-6 and H-14 to the nonprotonated olefinic carbon C-12, were located in the position of a double bond between C-12 and C-13. In addition, HMBC correlations from the oxymethine proton H-14 to C-6, C-12, and C-18 confirmed the hydroxy-substituent at C-14. Large coupling

constants between H-2 and H-3 ($J = 15.3$ Hz), as well as H-4 and H-5 ($J = 15.1$ Hz), showed the *E*-geometry of two double bonds at C-2 and C-4. The relative configuration of **4** was determined by a NOESY spectrum. NOE correlations from H-5 to H-7, H-14, H₃-16, and H₃-17 placed them on the same face of the molecule, whereas correlations from H-8 to H-10 indicated these protons were on the other side. To clarify the absolute configuration of **4**, the ECD spectra of minimum energy conformers by the TDDFT method at BH&HLYP/TZVP and CAM-B3LYP/TZVP levels were calculated, and the experimental ECD spectrum of **4** matched well with that of the calculated spectrum for (6*R*, 7*R*, 8*R*, 10*S*, 14*S*, and 15*R*)-**4** (Figures 6 and S59).

Table 2. ¹H and ¹³C NMR data of compounds **4–6** in DMSO-*d*₆.

No.	4		5		6	
	δ_C , Type	δ_H (J in Hz)	δ_C , Type	δ_H (J in Hz)	δ_C , Type	δ_H (J in Hz)
1	167.6, C		167.7, C		167.8, C ^a	
2	120.6, CH	5.80, d (15.3)	120.4, CH	5.77, d (15.2)	120.7, CH	5.79, d (15.3)
3	144.2, CH	7.13, dd (15.3, 10.8)	144.4, CH	7.14, dd (15.2, 11.1)	144.0, CH	7.11, dd (15.3, 11.0)
4	128.8, CH	6.23, dd (15.1, 10.8)	129.2, CH	6.29 dd (15.3, 11.1)	129.3, CH	6.31, dd (15.3, 11.0)
5	144.9, CH	6.11, dd (15.1, 9.3)	148.9, CH	5.95, overlap	148.9, CH	6.00, dd (15.3, 9.4)
6	43.6, CH	2.52, ddd (10.9, 9.3, 2.3)	49.4, CH	2.53, m	49.5, CH	2.52, m
7	49.4, CH	1.39, dd (10.9, 7.5)	43.6, CH	1.19, m	43.1, CH	1.29, overlap
8	34.5, CH	1.48, overlap	34.6, CH	1.41, overlap	39.2, CH	1.57, dd (12.3, 2.9)
9	44.7, CH ₂	1.70, m 0.89, m	48.7, CH ₂	1.41, overlap 0.98, m	39.5, CH ₂	1.29, overlap 0.73, q (12.3)
10	36.3, CH	1.48, overlap	68.0, C	1.62, overlap	36.1, CH	1.71, m
11	44.0, CH ₂	2.14, ddd (12.1, 3.8, 1.8) 1.59, m	41.9, CH ₂	1.41, overlap	32.4, CH ₂	α 1.15, overlap β 1.52, m
12	138.8, C		37.6, CH	1.62, overlap	42.2, CH	1.15, overlap
13	124.2, CH	5.31, d (2.0)	75.2, CH	3.33, m	65.5, CH	3.66, d (6.0)
14	68.7, CH	3.59, m	124.1, CH	5.95, overlap	127.1, CH	5.74, dt (6.0, 1.5)
15	36.2, CH	1.48, overlap	139.1, C		136.1, C	
16	15.6, CH ₃	0.90, d (6.8)	22.0, CH ₃	1.58, s	21.9, CH ₃	1.52, s
17	20.4, CH ₃	0.92, d (6.3)	21.5, CH ₃	0.81, d (6.6)	22.1, CH ₃	0.88, d (5.9)
18	22.1, CH ₃	0.87, d (6.5)	31.5, CH ₃	1.08, s	68.7, CH ₂	3.82, d (6.4)
13-OCH ₃			55.8, CH ₃	3.22, s		
19					170.4, C	
20					20.7, CH ₃	2.00, s
1-COOH				12.12, br s		

^a Detected by HMBC correlations.

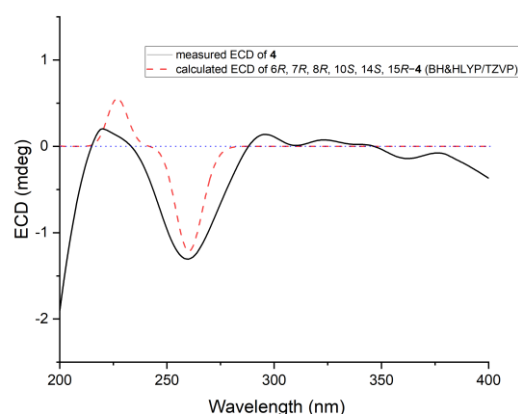


Figure 6. Experimental and calculated ECD of compound **4**.

Compound **5** was obtained as a white amorphous powder, and the molecular formula was assigned as C₁₉H₂₈O₄ by HRESIMS data. Detailed analysis of the ¹H and ¹³C data (Table 2) showed that it was similar to tanzawaic acid U [17] except that resonances for the methine unit at δ_C 32.3 and δ_H 1.46 (CH-10) in tanzawaic acid U were replaced by an

oxygenated/nonprotonated carbon at δ_C 68.0 (C-10) in **5**. These observations were further supported by relevant COSY and HMBC correlations (Figure 2). The coupling constants of two double bonds at C-2 and C-4 were 15.2 and 15.3 Hz, respectively, suggesting *E*-geometry for the double bonds. NOE correlations from H-5 to H-7 and H₃-17, as well as from H₃-17 to H₃-18, indicated the same orientation of these protons, while correlations from H-6 to H-12 and H-13 showed them on the opposite side. The absolute configuration of **5** was determined by both ECD calculation and comparisons with known compounds **9** and **10**. The experimental ECD spectrum of **5** aptly matched the calculated spectra of (6*R*, 7*R*, 8*R*, 10*R*, 12*S*, 13*S*)-**5** at BH&HLYP/TZVP, CAM-B3LYP/TZVP, and PBE0/TZVP levels (Figure 7 and Figure S59). Besides, **5** showed a positive Cotton effect at approximately 264 nm similar to that of compounds **9** and **10** (Figure 8), which also confirmed the absolute configuration of **5**. Compound **5** was named 10-hydroxytanzawaic acid U.

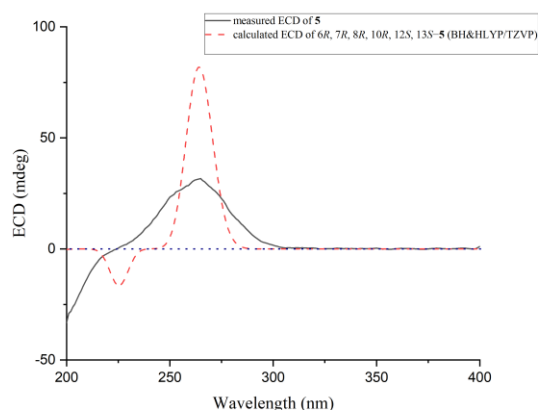


Figure 7. Experimental and calculated ECD of compound **5**.

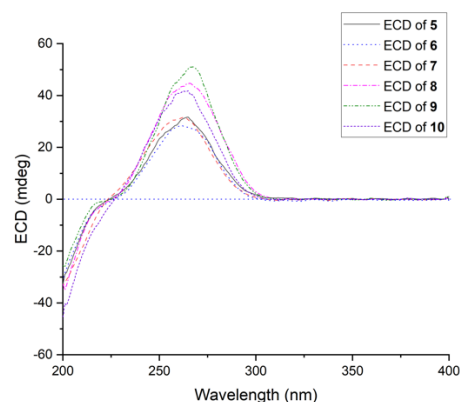


Figure 8. Experimental ECD of compounds **5–10**.

Compound **6** was isolated as a white amorphous powder and assigned the molecular formula $C_{20}H_{28}O_5$ by negative HRESIMS data. A detailed comparison of the NMR spectral data (Table 2) with the known compound tanzawaic acid R [17] suggested that they were very similar. However, signals for a carboxyl carbon at δ_C 170.4 and a methyl group at δ_C/δ_H 20.7/2.00 related to an acetoxy group were observed in the NMR spectra of **6**. HMBC correlations from H₂-18 to C-9, C-11, and C-19 as well as H₃-20 to C-19 placed the acetoxy group at C-18 (Figure 2). Large coupling constants between H-2 and H-3, as well as between H-4 and H-5 ($J = 15.3$ Hz), indicated the *E*-geometry of two double bonds. NOESY correlations from H₃-17 to H-5, H-7, and H₂-18, as well as from H₂-18 to H-11 β , suggested the same orientation of these protons, while correlations from H-12 to H-8 and H-10 as well as from H-13 to H-11 α placed these groups on the opposite face. From the ECD data and biogenetic considerations, the absolute configuration of compound **6** was

assigned as 6*R*, 7*R*, 8*R*, 10*S*, 12*S*, and 13*S*. Compound **6** was named 18-*O*-acetyltanzawaic acid **R**.

Steckwaic acid I (**7**) was obtained as a white amorphous powder, and the molecular formula was assigned as C₁₉H₂₈O₄ by analysis of the HRESIMS data. A detailed comparison of the NMR spectral data between **7** (Table 3) and tanzawaic acid **S** (**10**) [17] suggested that they were very similar, except the coupling constant between H-4 and H-5 ($J = 11.1$ Hz) in **7** was much smaller than that of **10** ($J_{4,5} = 15.3$ Hz), indicating the geometry of the double bond at C-4 changed from *E* in **10** to *Z* in **7**. The planar structure was further determined by COSY and HMBC correlations (Figure 2), and the relative configuration was confirmed by the NOESY spectrum. The NOESY correlations from H-5 to H-7 and H₃-17 showed these groups to be on the same side, whereas correlations from H-6 to H-8, H-12, and H-13, as well as from H-10 to H-8 and H-12, indicated the opposite side of these protons. The absolute configuration of **7** was confirmed by comparing the ECD spectrum with those of known compounds **9** and **10**. The same positive Cotton effects around 265 nm demonstrated consistent absolute configurations with those of 6*R*, 7*R*, 8*R*, 10*S*, 12*S*, and 13*S*.

Table 3. ¹H and ¹³C NMR data of compounds **7** and **8** in DMSO-*d*₆.

No.	7		8	
	δ_C , Type	δ_H (J in Hz)	δ_C , Type	δ_H (J in Hz)
1	168.8, C ^a		168.2, C	
2	123.9, CH	5.82, d (15.4)	121.2, CH	5.80, d (15.3)
3	141.8, CH	7.01, dd (15.4, 11.1)	144.5, CH	7.12, dd (15.3, 11.0)
4	129.6, CH	6.22, td (11.1, 5.2)	129.6, CH	6.28, dd (15.3, 11.0)
5	146.6, CH	5.78, dd (11.1, 5.2)	149.0, CH	5.94, dd (15.3, 9.2)
6	49.5, CH	2.53, m	49.6, CH	2.57, t (9.2)
7	40.0, CH	1.57, overlap	48.7, CH	0.99, m
8	42.1, CH	1.23, overlap	39.2, CH	1.37, overlap
9	39.2, CH ₂	1.23, overlap	40.0, CH ₂	1.61, d (12.5)
10	39.5, CH	0.63, dd (12.2, 5.6)	39.2, CH	0.70, q (12.5)
11	32.8, CH ₂	1.46, m	32.9, CH ₂	1.37, overlap
12	44.3, CH	1.57, overlap	43.8, CH	α 2.17, d (12.3)
13	75.3, CH	1.07, m	80.3, CH	β 0.57, q (12.3)
14	123.9, CH	1.23, overlap	126.3, CH	1.10, m
15	139.4, C	3.37, d (6.1)	134.7, C	3.32, d (9.4)
16	22.0, CH ₃	5.91, d (6.1)	126.3, CH	5.64, m
17	22.0, CH ₃	1.58, s	21.9, CH ₃	1.55, s
18	66.6, CH ₂	0.87, d (6.5)	22.9, CH ₃	0.87, d (6.5)
13-OCH ₃	55.8, CH ₃	3.18, d (6.1)	66.9, CH ₂	3.19, d (6.2)
18-OH		3.22, s	55.7, CH ₃	3.26, s
				4.35, br s

^a Detected by HMBC correlations.

Compound **8** was also obtained as a white amorphous powder with the molecular formula C₁₉H₂₈O₄ as measured by HRESIMS. Analysis of ¹H and ¹³C NMR data (Table 3) showed similarities to those reported for tanzawaic acid **S** (**10**) that were measured in methanol-*d*₄ [17] and our isolates that were measured in DMSO-*d*₆ (Experimental section). The primary differences between **8** and **10** were the signals of an oxygenated methine at δ_C/δ_H 80.3/3.32 (CH-13) in **8** replaced by signals at δ_C/δ_H 75.3/3.37 (CH-13) in **10**, revealing the configuration at C-13 had been changed. This deduction was further supported by the relevant COSY and HMBC correlations shown in Figure 2, as well as NOESY data shown in Figure 3. NOE correlations from H-5 to H-7 and H₃-17, from H-7 to H-13, and from H₂-18 to H-11 β suggested they were on one side, whereas correlations from H-6 to H-8 and H-12 and from H-13-OCH₃ to H-10 and H-11 α placed them on another face. By comparing

the ECD spectrum with that of compounds **9** and **10**, the absolute configuration of **8** was assigned as 6*R*, 7*R*, 8*R*, 10*S*, 12*S*, and 13*R*. Compound **8** was named 13*R*-tanzawaic acid S.

In addition to the new compounds **1–8**, two structurally related known analogues **9** and **10** were also isolated, and their structures were identified as tanzawaic acid H (**9**) and tanzawaic acid S (**10**) based on the comparison of NMR data, optical rotations, and ECD spectra with those described in literature reports [16,17].

The absolute configurations of major chiral centers for compounds **1–10** are consistent except for position C-13. In comparison to 13*S* methoxy-substituent (compounds **5**, **7**, and **10**), the resonance of C-13 in the 13*R* isomer (compound **8**) shifted ~5 ppm downfield in the ¹³C NMR spectra. An analogous carbon (4.4 ppm) was observed for the analogous hydroxy-substituent when comparing compound **6** with compound **9**. Besides, for the compounds with the same absolute configuration at C-13 (**5**, **6**, **7**, and **10**), the methoxy-substituent (**5**, **7**, and **10**) could shift downfield approximately 10 ppm in the ¹³C NMR spectra compared to that of hydroxy-substituent (**6**).

Although some tanzawaic acid derivatives were tested for their cytotoxic [16] and lipid-lowering [17] activities, a few of them exhibited significant activities. Compounds **1–10** were assayed for their antibacterial activities against one human and nine aquatic pathogenic bacteria as well as seven plant-pathogenic fungi. Compound **8** showed moderate activity against the human pathogenic bacterium *Escherichia coli* with an MIC value of 8 µg/mL (the MIC value of the positive control chloramphenicol was 1 µg/mL), while compound **10** exhibited inhibitory activity against the aquatic pathogenic bacterium *Edwardsiella tarda* with an MIC value of 16 µg/mL (the MIC value of the positive control chloramphenicol was 2 µg/mL) (Table 4). The results suggested that the absolute configuration of C-13 influenced the antibacterial activities of different bacteria (**8** vs. **10**) as supported by the fact that compound **8** with a 13*R* configuration showed stronger activity against *E. coli* but weaker activity against *E. tarda*, while compound **10** with a 10*S* configuration showed stronger activity against *E. tarda* but no activity against *E. coli*. The geometry of the double bond at C-4 also affected the activity (**7** vs. **10**), revealed by the fact that the *E*-geometry (**10**) exhibited stronger activity against *E. tarda* while compound **7** with *Z*-geometry at C-4 did not show any activity. Other compounds did not exhibit antimicrobial activities (MIC > 64 µg/mL).

Table 4. Antibacterial activities of active compounds **5** and **8–10** (MIC, µg/mL) ^a.

	<i>E. tarda</i>	<i>E. coli</i>	<i>V. parahaemolyticus</i>	<i>V. vulnificus</i>
5	-	-	16	-
8	64	8	-	-
9	-	-	64	-
10	16	-	-	-
Chloramphenicol ^b	2	1	1	2

^a (-) = MIC > 64 µg/mL. ^b Chloramphenicol as positive control.

3. Materials and Methods

3.1. General Experimental Procedures

General experimental procedures were the same as previously reported [19,20].

3.2. Fungal Material

The fungal strain *Penicillium steckii* AS-324 was obtained from fresh tissues of *Acanthogorgia* sp., which were collected from Magellan seamount. Taxonomic identification of the fungus was accomplished by comparing its ITS region sequence to that of *Penicillium steckii* (MT582790.1), which showed 99.64% similarity. The sequence data of the fungus AS-324 were submitted and deposited in GenBank with the accession no. OK605032. The fungal strain is preserved at the Key Laboratory of Experimental Marine Biology, Institute of Oceanology, Chinese Academy of Sciences (IOCAS, Qingdao, China).

3.3. Fermentation, Extraction, and Isolation

For chemical investigations, the fresh mycelia of *P. steckii* AS-324 were grown on PDA medium at 28 °C for five days and were then inoculated into 125 × 1 L Erlenmeyer flasks with rice solid medium (70 g rice, 0.1 g corn syrup, 0.3 g peptone, 0.1 g methionine, and 100 mL naturally sourced and filtered seawater that was obtained from the Huiquan Gulf of the Yellow Sea near the campus of IOCAS), and statically cultured for 30 days at room temperature. After incubation, the fermented rice substrate was extracted three times with EtOAc. The combined EtOAc extracts were filtered and evaporated under reduced pressure to yield organic extract (120 g), which was subjected to vacuum liquid chromatography (VLC) eluting with different solvents of increasing polarity from petroleum ether (PE) to MeOH to yield nine fractions (Frs. 1–9). Fr. 6 (11 g), eluted with PE–EtOAc (1:1), was purified by column chromatography (CC) over Lobar LiChroprep RP-18 with a MeOH–H₂O gradient (from 10:90 to 100:0) to afford seven subfractions (Frs. 6.1–6.7). Fr. 6.4 (eluted with MeOH–H₂O, 40:60, 260 mg) was further purified by CC on Si gel eluting with a CH₂Cl₂–MeOH gradient (from 100:1 to 20:1) to gain Frs. 6.4.1–6.4.3. Fr. 6.4.1 was further purified by prep. TLC (plate: 20 × 20 cm, developing solvents: PE–Acetone, 1:1) and Sephadex LH-20 (MeOH) to obtain compound **1** (42.3 mg). Fr. 6.4.2 was further purified by semi-preparative HPLC (Elite ODS-BP column, 10 μm; 20 × 250 mm; 50% MeOH–H₂O, 10 mL/min) to gain compounds **2** (15.6 mg, *t_R* = 15.5 min) and **4** (22.8 mg, *t_R* = 17.5 min). Fr. 6.4.3 was purified by prep. TLC (plate: 20 × 20 cm, developing solvents: CH₂Cl₂–Acetone, 3:1) and Sephadex LH-20 (MeOH) to obtain compound **3** (10.2 mg). Fr. 7 (5.5 g), eluted with CH₂Cl₂–MeOH (20:1), was purified by reverse-phase column chromatography (CC) over Lobar LiChroprep RP-18 with a MeOH–H₂O gradient (from 10:90 to 100:0) to yield five subfractions (Frs. 7.1–7.5). Fr. 7.3 (eluted with MeOH–H₂O, 50:50, 326 mg) was further purified by CC on Si gel eluting with a CH₂Cl₂–MeOH gradient (from 100:1 to 20:1), prep. TLC (plate: 20 × 20 cm, developing solvents: PE–Acetone, 1:1), and Sephadex LH-20 (MeOH) to obtain compounds **5** (3.0 mg) and **10** (38.7 mg). Fr. 7.4 (eluted with MeOH–H₂O, 60:40, 118 mg) was fractionated by CC on Si gel eluting with a CH₂Cl₂–MeOH gradient (from 80:1 to 20:1) and Sephadex LH-20 (MeOH) to afford compound **6** (20.4 mg). Fr. 8 (10.0 g), eluted with CH₂Cl₂/MeOH (10:1), was purified by reverse-phase CC over Lobar LiChroprep RP-18 with an MeOH–H₂O gradient (from 10:90 to 100:0) to yield three subfractions (Frs. 8.1–8.3). Fr. 8.1 (eluted with MeOH–H₂O 30:70) was further purified by CC on Si gel eluting with a CH₂Cl₂–MeOH gradient (from 100:1 to 50:1) and semi-preparative HPLC (Elite ODS-BP column, 10 μm; 20 × 250 mm; 60% MeOH–H₂O, 10 mL/min) to gain compounds **7** (13.2 mg, *t_R* = 18.7 min) and **9** (8.9 mg, *t_R* = 16.5 min). Fr. 8.3 (eluted with MeOH–H₂O 50:50) was further purified by CC on Si gel eluting with a CH₂Cl₂–MeOH gradient (from 100:1 to 50:1), prep. TLC (plate: 20 × 20 cm, developing solvents: PE–Acetone, 1:1), semi-preparative HPLC (Elite ODS-BP column, 10 μm; 20 × 250 mm; 45% MeOH–H₂O, 10 mL/min), and Sephadex LH-20 (MeOH) to obtain compound **8** (3.0 mg).

Steckwaic acid E (1): Colorless crystals (MeOH); mp 178–180 °C; $[\alpha]_D^{25} +56.0$ (*c* 0.25, MeOH); UV (MeOH) λ_{\max} (log ϵ) 217 (3.19) nm; ECD (0.95 mM, MeOH) λ_{\max} ($\Delta\epsilon$) 225 (+5.42) nm; ¹H and ¹³C NMR data, Table 1; ESIMS *m/z* 263 [M – H][–]; HRESIMS *m/z* 263.1657 [M – H][–] (calcd for C₁₆H₂₃O₃, 263.1653).

Steckwaic acid F (2): Colorless crystals; mp 242–244 °C; $[\alpha]_D^{25} +30.8$ (*c* 0.26, MeOH); UV (MeOH) λ_{\max} (log ϵ) 216 (3.12) nm; ECD (0.72 mM, MeOH) λ_{\max} ($\Delta\epsilon$) 223 (+4.17) nm; ¹H and ¹³C NMR data, Table 1; ESIMS *m/z* 277 [M – H][–]; HRESIMS *m/z* 277.1439 [M – H][–] (calcd for C₁₆H₂₁O₄, 277.1445).

Steckwaic acid G (3): White amorphous powder; $[\alpha]_D^{25} +67.9$ (*c* 0.28, MeOH); UV (MeOH) λ_{\max} (log ϵ) 213 (2.95) nm; ECD (0.95 mM, MeOH) λ_{\max} ($\Delta\epsilon$) 223 (+3.22), 295 (+0.53) nm; ¹H and ¹³C NMR data, Table 1; ESIMS *m/z* 263 [M – H][–]; HRESIMS *m/z* 263.1657 [M – H][–] (calcd for C₁₆H₂₃O₃, 263.1653).

Steckwaic acid H (4): Colorless oil; $[\alpha]_D^{25} -34.5$ (*c* 0.29, MeOH); UV (MeOH) λ_{\max} (log ϵ) 260 (3.00) nm; ECD (0.34 mM, MeOH) λ_{\max} ($\Delta\epsilon$) 220 (+0.19), 295 (+0.16) nm; ¹H and ¹³C

NMR data, Table 2; ESIMS m/z 289 $[M - H]^-$; HRESIMS m/z 289.1809 $[M - H]^-$ (calcd for $C_{18}H_{25}O_3$, 289.1809).

10-Hydroxytanzawaic acid U (5): White amorphous powder; $[\alpha]_D^{25} +50.0$ (c 0.10, MeOH); UV (MeOH) λ_{max} (log ϵ) 265 (3.08) nm; ECD (1.56 mM, MeOH) λ_{max} ($\Delta\epsilon$) 264 (+6.12) nm; 1H and ^{13}C NMR data, Table 2; ESIMS m/z 319 $[M - H]^-$; HRESIMS m/z 319.1908 $[M - H]^-$ (calcd for $C_{19}H_{27}O_4$, 319.1915).

18-O-Acetyltanzawaic acid R (6): White amorphous powder; $[\alpha]_D^{25} +82.5$ (c 0.40, MeOH); UV (MeOH) λ_{max} (log ϵ) 265 (3.32) nm; ECD (0.72 mM, MeOH) λ_{max} ($\Delta\epsilon$) 261 (+12.0) nm; 1H and ^{13}C NMR data, Table 2; ESIMS m/z 347 $[M - H]^-$; HRESIMS m/z 347.1861 $[M - H]^-$ (calcd for $C_{20}H_{27}O_5$, 347.1864).

Steckwaic acid I (7): White amorphous powder, $[\alpha]_D^{25} +165.2$ (c 0.23, MeOH); UV (MeOH) λ_{max} (log ϵ) 263 (3.27) nm; ECD (0.78 mM, MeOH) λ_{max} ($\Delta\epsilon$) 262 (+12.2) nm; 1H and ^{13}C NMR data, Table 3; ESIMS m/z 319 $[M - H]^-$; HRESIMS m/z 319.1908 $[M - H]^-$ (calcd for $C_{19}H_{27}O_4$, 319.1915).

13R-Tanzawaic acid S (8): Colorless solid; $[\alpha]_D^{25} +254.5$ (c 0.22, MeOH); UV (MeOH) λ_{max} (log ϵ) 265 (3.50) nm; ECD (0.78 mM, MeOH) λ_{max} ($\Delta\epsilon$) 266 (+17.4) nm; 1H and ^{13}C NMR data, Table 3; ESIMS m/z 319 $[M - H]^-$; HRESIMS m/z 319.1912 $[M - H]^-$ (calcd for $C_{19}H_{27}O_4$, 319.1915).

Tanzawaic acid S (10): Colorless solid; $[\alpha]_D^{25} +76.9$ (c 0.13, MeOH); UV (MeOH) λ_{max} (log ϵ) 264 (3.39) nm; ECD (0.86 mM, MeOH) λ_{max} ($\Delta\epsilon$) 263 (+14.7) nm; 1H NMR data (DMSO- d_6) δ_H : 5.80 (1H, m, H-2), 7.12 (1H, dd, $J = 14.5, 10.9$ Hz, H-3), 6.27 (1H, dd, $J = 15.3, 10.9$ Hz, H-4), 5.93 (2H, m, H-5, H-14), 2.54, (1H, m, H-6), 1.23 (3H, m, H-7, H-10, H-12), 0.63 (1H, m, H-8), 1.59 (2H, m, H-9a, H-11a), 1.45 (1H, m, H-9b), 1.08 (1H, m, H-11b), 3.37 (1H, dd, $J = 6.1, 1.8$ Hz, H-13), 1.57, (3H, s, H₃-16), 0.87 (3H, d, $J = 6.5$ Hz, H₃-17), 3.19 (2H, d, $J = 6.2$ Hz, H₂-18), 3.22 (3H, s, H₃-13-OCH₃); ^{13}C NMR data (DMSO- d_6) δ_C : 170.0 (C, C-1), 120.8 (CH, C-2), 143.7 (CH, C-3), 129.2 (CH, C-4), 148.4 (CH, C-5), 49.5 (CH, C-6), 44.2 (CH, C-7), 39.2 (CH, C-8), 39.5 (CH₂, C-9), 40.0 (CH, C-10), 32.7 (CH₂, C-11), 42.1 (CH, C-12), 75.3 (CH, C-13), 124.0 (CH, C-14), 139.1 (C, C-15), 22.0 (CH₃, C-16), 21.9 (CH₃, C-17), 66.6, (CH₂, C-18), 55.8 (CH₃, C-13-OCH₃); ESIMS m/z 319 $[M - H]^-$; HRESIMS m/z 319.1914 $[M - H]^-$ (calcd for $C_{19}H_{27}O_4$, 319.1915).

3.4. X-ray Crystallographic Analysis of Compounds 1 and 2

Colorless crystals of compounds **1** and **2** were obtained from the solution of MeOH. Crystallographic data were collected on a Bruker D8 Venture diffractometer equipped with a graphite-monochromatic Cu K α radiation ($\lambda = 1.54178$) Å at 173 K [21]. The data were corrected for absorption by using the program SADABS [22]. The structures were solved by direct methods with the SHELXTL software package [23,24]. All non-hydrogen atoms were refined anisotropically. The H atoms connected to C atoms were calculated theoretically, and those to O atoms were assigned by difference Fourier maps. The absolute structures were determined by refinement of the Flack parameter [25]. The structures were optimized by full-matrix least-squares techniques.

Crystal data for compound 1: $C_{16}H_{24}O_3$, F.W. = 264.35, monoclinic space group $P2(1)$, unit cell dimensions $a = 5.7450(10)$ Å, $b = 12.778(3)$ Å, $c = 10.226(3)$ Å, $V = 749.3(3)$ Å³, $\alpha = \gamma = 90^\circ$, $\beta = 93.424(14)$, $Z = 2$, $d_{calcd} = 1.172$ mg/m³, crystal dimensions $0.200 \times 0.180 \times 0.160$ mm, $\mu = 0.632$ mm⁻¹, $F(000) = 288$. The 2734 measurements yielded 2464 independent reflections after equivalent data were averaged. The final refinement gave $R_1 = 0.0421$ and $wR_2 = 0.1125$ [$I > 2\sigma(I)$]. The absolute structure parameter was $-0.09(13)$.

Crystal data for compound 2: $C_{16}H_{22}O_4$, F.W. = 278.33, orthorhombic space group $P2(1)2(1)2(1)$, unit cell dimensions $a = 5.18970(10)$ Å, $b = 11.7476(2)$ Å, $c = 24.0950(5)$ Å, $V = 1468.99(5)$ Å³, $\alpha = \beta = \gamma = 90^\circ$, $Z = 4$, $d_{calcd} = 1.259$ mg/m³, crystal dimensions $0.180 \times 0.160 \times 0.140$ mm, $\mu = 0.727$ mm⁻¹, $F(000) = 600$. The 2681 measurements yielded 2409 independent reflections after equivalent data were averaged. The final refinement gave $R_1 = 0.0371$ and $wR_2 = 0.0956$ [$I > 2\sigma(I)$]. The absolute structure parameter was $0.05(10)$.

3.5. Computational Section

Conformational searches were performed via molecular mechanics using the MMFF method in MacroModel software, and the geometries were reoptimized at the B3LYP/6-31G(d) PCM/MeOH level using Gaussian 09 software to obtain the energy-minimized conformers [26]. Then, the optimized conformers were subjected to calculate the ECD spectra using TDDFT at the BH&HLYP/TZVP, CAM-B3LYP/TZVP, and PBE0/TZVP levels. The solvent effects of the MeOH solution were evaluated at the same DFT level using the SCRF/PCM method.

3.6. Antimicrobial Assays

The antimicrobial activities against one human pathogenic bacterium (*Escherichia coli* EMBLC-1), nine aquatic pathogens (*Aeromonas hydrophilia* QDIO-1, *E. tarda* QDIO-2, *Micrococcus luteus* QDIO-3, *Pseudomonas aeruginosa* QDIO-4, *Vibrio alginolyticus* QDIO-5, *V. anguillarum* QDIO-6, *V. harveyi* QDIO-7, *V. parahaemolyticus* QDIO-8, and *V. vulnificus* QDIO-10), as well as seven plant-pathogenic fungi (*Alternaria solani* QDAU-1, *Colletotrichum gloeosporioides* QDAU-2, *Fusarium graminearum* QDAU-4, *F. oxysporum* QDAU-8, *Gaeumannomyces graminis* QDAU-21, *Rhizoctonia cerealis* QDAU-20, and *Valsa mali* QDAU-16), were determined by a serial dilution technique using 96-well microtiter plates [27]. The aquatic pathogenic strains and human pathogenic bacteria were obtained from IOCAS. Tested compounds and the positive control (chloramphenicol for bacteria and amphotericin B for fungi) were dissolved in DMSO to produce a stock solution.

4. Conclusions

In conclusion, eight new polyketide derivatives (1–8) and two related known analogues (9 and 10) were identified from the endozoic fungus *P. steckii* AS-324, which was obtained from the fresh tissues of deep-sea *Acanthogorgiidae* sp. coral collected from Magellan seamount in the Western Pacific Ocean at a depth of 1458 m. Compounds 1–3, with an acrylic acid side chain at C-4, have been rarely observed [28], and the double bond between C-12 and C-13 in compound 4 is a new observation. Antimicrobial activities of compounds 1–10 were tested, and compound 8 showed potent activity against *E. coli* with an MIC value of 8 µg/mL while compound 10 exhibited inhibitory activity against *E. tarda* with an MIC value of 16 µg/mL.

Supplementary Materials: The following supporting information can be downloaded at: <https://www.mdpi.com/article/10.3390/ijms23116332/s1>.

Author Contributions: Conceptualization, X.-Y.H., L.-H.M. and B.-G.W.; NMR data collection, X.-M.L.; experiment and analysis, X.-Y.H.; writing—original draft preparation, X.-Y.H.; writing—review and editing, L.-H.M. and B.-G.W.; funding acquisition and project administration, B.-G.W. All authors have read and agreed to the published version of the manuscript.

Funding: This research was funded by the National Natural Science Foundation of China (U2006203 and 41976090), the Natural Science Foundation of Jiangsu province (BK20201211), and the Senior User Project of RV *KEXUE* (KEXUE2020GZ02).

Institutional Review Board Statement: Not applicable.

Informed Consent Statement: Not applicable.

Data Availability Statement: Not applicable.

Acknowledgments: B.-G.W. acknowledges the support of the RV *KEXUE* of the National Major Science and Technology Infrastructure from the Chinese Academy of Sciences (for sampling) and the Oceanographic Data Center at IOCAS (for CPU time).

Conflicts of Interest: The authors declare no conflict of interest.

References

1. Rothschild, L.J.; Mancinelli, R.L. Life in extreme environments. *Nature* **2001**, *409*, 1092–1101. [[CrossRef](#)] [[PubMed](#)]
2. Wright, P.C.; Westacott, R.E.; Burja, A.M. Piezotolerance as a metabolic engineering tool for the biosynthesis of natural products. *Biomol. Eng.* **2003**, *20*, 325–331. [[CrossRef](#)]
3. Sun, C.; Mudassir, S.; Zhang, Z.; Feng, Y.; Chang, Y.; Che, Q.; Gu, Q.; Zhu, T.; Zhang, G.; Li, D. Secondary metabolites from deep-sea derived microorganisms. *Curr. Med. Chem.* **2020**, *27*, 6244–6273. [[CrossRef](#)]
4. Skropeta, D.; Wei, L. Recent advances in deep-sea natural products. *Nat. Prod. Rep.* **2014**, *31*, 999–1025. [[CrossRef](#)] [[PubMed](#)]
5. Marchese, P.; Young, R.; O'Connell, E.; Afoullouss, S.; Baker, B.J.; Allcock, A.L.; Barry, F.; Murphy, J.M. Deep-sea coral garden invertebrates and their associated fungi are genetic resources for chronic disease drug discovery. *Mar. Drugs* **2021**, *19*, 390. [[CrossRef](#)]
6. Li, J.; Zhong, M.; Lei, M.; Xiao, S.; Li, Z. Diversity and antibacterial activities of culturable fungi associated with coral *Porites pukoensis*. *World J. Microbiol. Biotechnol.* **2014**, *30*, 2551–2558. [[CrossRef](#)]
7. Wei, X.; Feng, C.; Zhang, D.-M.; Li, X.-H.; Zhang, C.-X. New indole diketopiperazine alkaloids from soft coral-associated epiphytic fungus *Aspergillus* sp. EGF 15-0-3. *Chem. Biodivers.* **2020**, *17*, e2000106. [[CrossRef](#)]
8. Wang, L.; Huang, Y.; Zhang, L.; Liu, Z.; Liu, W.; Xu, H.; Zhang, Q.; Zhang, H.; Yan, Y.; Liu, Z.; et al. Structures and absolute configurations of phomalones from the coral-associated fungus *Parengyodontium album* sp. SCSIO 40430. *Org. Biomol. Chem.* **2021**, *19*, 6030–6037. [[CrossRef](#)]
9. Proksch, P.; Edrada, R.A.; Ebel, R. Drugs from the seas—current status and microbiological implications. *Appl. Microbiol. Biotechnol.* **2002**, *59*, 125–134.
10. Bao, J.; Sun, Y.-L.; Zhang, X.-Y.; Han, Z.; Gao, H.-C.; He, F.; Qian, P.-Y.; Qi, S.-H. Antifouling and antibacterial polyketides from marine gorgonian coral-associated fungus *Penicillium* sp. SCSGAF 0023. *J. Antibiot.* **2013**, *66*, 219–223. [[CrossRef](#)]
11. Chen, Y.; Mao, W.; Wang, J.; Zhu, W.; Zhao, C.; Li, N.; Wang, C.; Yan, M.; Guo, T.; Liu, X. Preparation and structural elucidation of a glucomannogalactan from marine fungus *Penicillium commune*. *Carbohydr. Polym.* **2013**, *97*, 293–299. [[CrossRef](#)] [[PubMed](#)]
12. Sun, K.; Chen, Y.; Niu, Q.; Zhu, W.; Wang, B.; Li, P.; Ge, X. An exopolysaccharide isolated from a coral-associated fungus and its sulfated derivative activates macrophages. *Int. J. Biol. Macromol.* **2016**, *82*, 387–394. [[CrossRef](#)] [[PubMed](#)]
13. Meng, L.-H.; Li, X.-M.; Zhang, F.-Z.; Wang, Y.-N.; Wang, B.-G. Talascortenes A–G, highly oxygenated diterpenoid acids from the sea-anemone-derived endozoic fungus *Talaromyces scorteus* AS-242. *J. Nat. Prod.* **2020**, *83*, 2528–2536. [[CrossRef](#)]
14. Chi, L.-P.; Li, X.-M.; Wan, Y.-P.; Li, X.; Wang, B.-G. Ophiobolin sesterterpenoids and farnesylated phthalide derivatives from the deep sea cold-seep-derived fungus *Aspergillus insuetus* SD-512. *J. Nat. Prod.* **2020**, *83*, 3652–3660. [[CrossRef](#)] [[PubMed](#)]
15. Yao, G.; Chen, X.; Zheng, H.; Liao, D.; Yu, Z.; Wang, Z.; Chen, J. Genomic and chemical investigation of bioactive secondary metabolites from a marine-derived fungus *Penicillium steckii* P2648. *Front. Microbiol.* **2021**, *12*, 600991. [[CrossRef](#)] [[PubMed](#)]
16. EI-Neketi, M.; Ebrahim, W.; Lin, W.; Gredara, S.; Badria, F.; Saad, H.A.; Lai, D.; Proksch, P. Alkaloids and polyketides from *Penicillium citrinum*, an endophyte isolated from the moroccan plant *Ceratonia siliqua*. *J. Nat. Prod.* **2013**, *76*, 1099–1104. [[CrossRef](#)]
17. Yu, G.; Wang, S.; Wang, L.; Che, Q.; Zhu, T.; Zhang, G.; Gu, Q.; Guo, P.; Li, D. Lipid-lowering polyketides from the fungus *Penicillium Steckii* HDN13-279. *Mar. Drugs* **2018**, *16*, 25. [[CrossRef](#)]
18. Hu, X.-Y.; Li, X.-M.; Wang, B.-G.; Meng, L.-H. Tanzawaic acid derivatives: Fungal polyketides from the deep-sea coral-derived endozoic *Penicillium steckii* AS-324. *J. Nat. Prod.* **2022**, *85*, 1398–1406. [[CrossRef](#)]
19. Cao, J.; Li, X.-M.; Li, X.; Li, H.-L.; Konuklugil, B.; Wang, B.-G. Uncommon N-methoxyindole-diketopiperazines from *Acrostalagmus luteoalbus*, a marine algal isolate of endophytic fungus. *Chin. J. Chem.* **2021**, *39*, 2808–2814. [[CrossRef](#)]
20. Hu, X.-Y.; Wang, C.-Y.; Li, X.-M.; Yang, S.-Q.; Li, X.; Wang, B.-G.; Si, S.-Y.; Meng, L.-H. Cytochalasin derivatives from the endozoic *Curvularia verruculosa* CS-129, a fungus isolated from the deep-sea squat lobster *Shinkaia crosnieri* living in the cold seep environment. *J. Nat. Prod.* **2021**, *84*, 3122–3130. [[CrossRef](#)]
21. Crystallographic data of compounds 1 and 2 have been deposited in the Cambridge Crystallographic Data Centre as CCDCs 2130113 and 2143070, respectively. Hu Xueyi. Cambridge Crystallographic Data Centre. Available online: <http://www.ccdc.cam.ac.uk/datarequest/cif> (accessed on 29 April 2022).
22. Sheldrick, G.M. *SADABS, Software for Empirical Absorption Correction*; University of Göttingen: Göttingen, Germany, 1996.
23. Sheldrick, G.M. *SHELXL, Structure Determination Software Programs*; Bruker Analytical X-ray System Inc.: Madison, WI, USA, 1997.
24. Sheldrick, G.M. *SHELXL, Program for the Refinement of Crystal Structures*; University of Göttingen: Göttingen, Germany, 2014.
25. Parsons, S.; Flack, H.D.; Wagner, T. Use of intensity quotients and differences in absolute structure refinement. *Acta Crystallogr. Sect. B Struct. Sci. Cryst. Eng. Mater.* **2013**, *B69*, 249–259. [[CrossRef](#)] [[PubMed](#)]
26. Frisch, M.J.; Trucks, G.W.; Schlegel, H.B.; Scuseria, G.E.; Robb, M.A.; Cheeseman, J.R.; Scalmani, G.; Barone, V.; Mennucci, B.; Petersson, G.A.; et al. *Gaussian 09, Revision D.01*; Gaussian, Inc.: Wallingford, CT, USA, 2013.
27. Pierce, C.G.; Uppuluri, P.; Tristan, A.R.; Wormley, F.L., Jr.; Mowat, E.; Ramage, G.; Lopez-Ribot, J.L. A simple and reproducible 96-well plate-based method for the formation of fungal biofilms and its application to antifungal susceptibility testing. *Nat. Protoc.* **2008**, *3*, 1494–1500. [[CrossRef](#)] [[PubMed](#)]
28. Chen, C.-M.; Chen, W.-H.; Tao, H.-M.; Yang, B.; Zhou, X.-F.; Luo, X.-W.; Liu, Y.-H. Diversified polyketides and nitrogenous compounds from the mangrove endophytic fungus *Penicillium steckii* SCSIO 41025. *Chin. J. Chem.* **2021**, *39*, 2132–2140. [[CrossRef](#)]